

Near threshold production of the η meson via the quasi-free $pn \rightarrow pn\eta$ reaction

P. Moskal ^{a,b,*}, R. Czyżykiewicz ^a, H.-H. Adam ^c, S. D. Bass ^d,
 A. Budzanowski ^e, E. Czerwiński ^{a,b}, D. Gil ^a, D. Grzonka ^b,
 M. Janusz ^{a,b}, L. Jarczyk ^a, T. Johansson ^f, B. Kamys ^a,
 A. Khoukaz ^c, K. Kilian ^b, P. Klaja ^{a,b}, J. Majewski ^{a,b},
 W. Oelert ^b, C. Piskor-Ignatowicz ^a, J. Przerwa ^{a,b}, B. Rejdych ^a,
 J. Ritman ^b, T. Rożek ^g, T. Sefzick ^b, M. Siemaszko ^g,
 M. Silarski ^a, J. Smyrski ^a, A. Täschner ^c, M. Wolke ^b,
 P. Wüstner ^b, M. J. Zieliński ^a, W. Zipper ^g, J. Zdebik ^a

^a*Institute of Physics, Jagiellonian University, PL-30-059 Cracow, Poland*

^b*IKP & ZEL, Forschungszentrum Jülich, D-52425 Jülich, Germany*

^c*IKP, Westfälische Wilhelms-Universität, D-48149 Münster, Germany*

^d*Institute for Theoretical Physics, University of Innsbruck, Austria*

^e*Institute of Nuclear Physics, PL-31-342 Cracow, Poland*

^f*Department of Physics and Astronomy, Uppsala University, Sweden*

^g*Institute of Physics, University of Silesia, PL-40-007 Katowice, Poland*

Abstract

Total cross sections for the quasi-free $pn \rightarrow pn\eta$ reaction in the range from the kinematical threshold up to 20 MeV excess energy have been determined. At threshold they exceed corresponding cross sections for the $pp \rightarrow pp\eta$ reaction by a factor of about three in contrast to the factor of six established for higher excess energies. To large extent, the observed decrease of the ratio $\sigma(pn \rightarrow pn\eta)/\sigma(pp \rightarrow pp\eta)$ towards threshold may be assigned to the different energy dependence of the proton-proton and proton-neutron final state interactions.

The experiment has been conducted using a proton beam of the cooler synchrotron COSY and a cluster jet deuteron target. The proton-neutron reactions were tagged by the spectator proton whose momentum was measured for each event. Protons and neutron outgoing from the $pn \rightarrow pn\eta$ reaction have been registered by means of the COSY-11 facility, an apparatus dedicated for threshold meson production.

Key words: Meson production, isospin dependence, final state interaction

1 Introduction

In recent years meson production has been extensively studied in the context of understanding of the strong interaction in the non-perturbative energy domain of the quantum chromodynamics, where it is not obvious whether hadronic or quark-gluon degrees of freedom are more appropriate for the description of the dynamics and interaction of hadrons. For the η meson precise data [1,2,3,4,5,6,7] of the total cross section of the $pp \rightarrow pp\eta$ reaction allowed one to conclude that the reaction proceeds predominantly through the excitation of one of the protons to the $S_{11}(1535)$ state which subsequently de-excites via emission of the η meson. The crucial observations were a large value of the absolute cross section (about forty times larger than for the η' meson [8]) and isotropic angular distributions [5,7,9] of the η meson emission in the reaction center-of-mass system.

However, due to the negligible variation of the production amplitude in the range of few tens of MeV the full information available from the excitation function is reduced to a single number [10]. Consequently, measurements of one reaction channel are not sufficient to establish contributions from different production currents (e.g. mesonic, nucleonic, resonance or gluonic [11,12,13,14]). For this purpose, an exploration of isospin and spin degrees of freedom is mandatory. The first measurement of the dependence of the η production on the isospin of the interacting nucleons was conducted by the WASA/PROMICE collaboration [15] in the excess energy range from 16 MeV to 109 MeV. On the hadronic level, the observed strong isospin dependence indicated a dominant contribution to the production process from the isovector meson exchange. Further comparison of predictions involving exchanges of various mesons [11,12] with recent results on the analysing power [16] signified the dominance of the π meson exchange in the production process (though with a rather low statistical significance) [16]. This observation is in line with predictions of Nakayama et al. [12] and with calculations of Shyam [17]. Yet, it seems to be contra-intuitive due to the very large momentum transfer between the interacting nucleons needed to create the η meson near threshold which should rather favor exchanges of heavier mesons (e.g. ρ) as anticipated by authors of references [11,18]. Moreover, with the high momentum transfer a

* Corresponding author. Correspondence address: Institute of Physics, Jagiellonian University, ul. Reymonta 4, PL-30-059 Cracow, Poland.

Email address: p.moskal@fz-juelich.de (P. Moskal).

direct role of quarks and gluons in the production process is also conceivable. According to the Heisenberg uncertainty relation the distance probed by the $NN \rightarrow NN\eta$ reactions at threshold is expected to be about 0.26 fm. Geometrical considerations presented by Maltman and Isgur [19] indicate that at distances smaller than 2 fm the inter-nucleon potential should begin to be free of meson exchange effects and may be dominated by residual colour forces [19]. In particular, since the singlet components of the η and η' mesons couple to glue, it is natural to consider a mechanism where glue is excited in the “short distance” (~ 0.2 fm) interaction region of a proton-nucleon collision and then evolves to become an η or η' in the final state. Such gluonic induced production, proposed by Bass [13], is extra to the contributions associated with meson exchange models, and appears as a contact term in the axial U(1) extended chiral Lagrangian for low-energy QCD.

In order to verify the different production mechanisms it is of crucial importance to provide an empirical base with spin and isospin dependence of the cross sections of the near threshold meson production in the collision of nucleons as well as in the photo-production processes. Therefore, such investigations are conducted at several experimental facilities [20,21,22,23,24]. In this article we report on the measurement which enables us for the first time to determine cross sections for the $pn \rightarrow pn\eta$ reaction close to the kinematical threshold where a contribution from only a single partial wave is expected.

2 Experimental method

Measurements of the quasi-free $pn \rightarrow pn\eta$ reaction have been performed at the cooler synchrotron COSY [25] at the Research Center Jülich in Germany by means of the COSY-11 detector setup [26] presented schematically in Fig. 1. The proton beam with a nominal momentum of $p_{beam} = 2.075$ GeV/c, (corresponding to the kinetic energy of $T = 1.339$ GeV) was circulating through the deuteron cluster jet target [27] with an areal density of about 10^{14} atoms/cm². Due to the relatively weak binding energy of the deuteron (~ 2.2 MeV) which is by more than two orders of magnitude smaller than the kinetic energy of the bombarding protons and due to the relatively large average distance between the proton and the neutron (~ 3 fm [28]), it is quite probable that the beam proton interacts with the nucleon from the deuteron as if it would be a free particle. Such quasi-free proton-neutron interactions were tagged by the registration of the low energy proton moving upstream the beam. In the analysis the proton emerging from the deuteron is considered as a spectator which leaves the interaction region with the Fermi momentum undisturbed by the final state interaction with the other reaction products. In this approach we assume that the measured spectator proton was on its mass shell already at the collision moment and that the matrix element for the

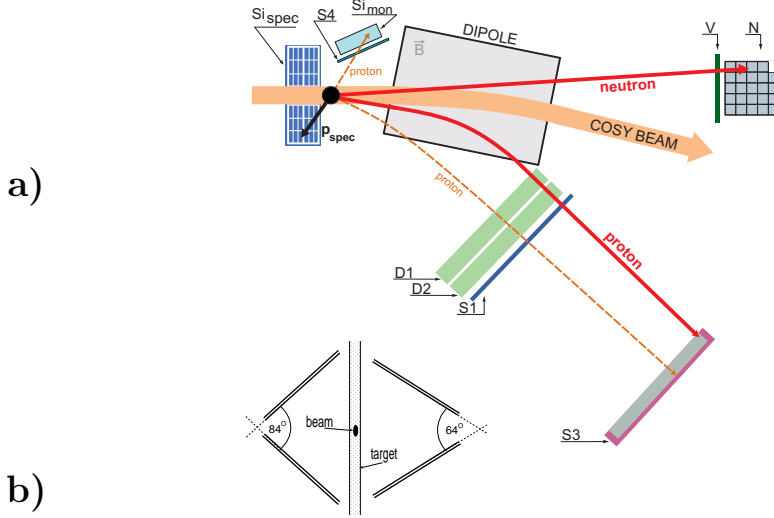


Fig. 1. (a) Schematic view of the COSY-11 detection setup [26]. D1 and D2 represent drift chambers. S1, S3, S4 denote scintillator counters. N stands for the neutral particle detector and V for the veto counter. Si_{mon} and Si_{spec} are silicon strip detectors used for the detection of the elastically scattered protons and spectator protons, respectively. Superimposed solid lines indicate correspondingly spectator proton, neutron and forward scattered proton from the quasi-free $pd \rightarrow p_{sp}pn\eta$ reaction and the dashed lines show an example of the quasi-free elastically scattered protons used for the monitoring of the luminosity. The size of detectors and their relative distances are not to scale. (b) Projection of the arrangement of the spectator detector as seen along the beam axis. The beam is moving in the direction perpendicular to the plane of the projection, while the target deuterons are moving from the bottom to the top.

production of the η meson by the beam proton off the neutron bound in the deuteron is identical to that for the free $pn \rightarrow pn\eta$ reaction. This assumption is supported by a theoretical investigation [29] and was already confirmed by various experiments [4,20,21,24,30]. In particular it was proven that even in the case of the pion production it is valid up to a Fermi momentum of 150 MeV/c [20].

The Fermi motion of nucleons causes the smearing of the total center-of-mass energy for the proton-neutron reaction ($\sqrt{s_{pn}}$). The resultant distribution of the excess energy for the quasi-free $pn \rightarrow pn\eta$ reaction ($Q \equiv \sqrt{s_{pn}} - m_p - m_n - m_\eta$) is broader than 50 MeV [7,23,31], and therefore to achieve an accuracy of Q in the order of a few MeV it is important to reconstruct the four-momentum vector of the interacting neutron on the event-by-event basis. Such an accuracy is mandatory for near threshold studies where the cross sections may vary by more than an order of magnitude within an excess energy range of a few tens of MeV [32]. Therefore, the spectator proton was registered not only to tag the quasi free proton-neutron reaction but also to determine the four-momentum vector of the reacting neutron. The usage of

the thin cluster target (10^{14} atoms/cm²) and mounting of the spectator detector inside the beam pipe ensured the negligible distortion of the momentum of the measured spectators. Based on the aforementioned spectator model and on the energy and momentum conservation, the four momentum of the target neutron $\mathbb{P}_t^n \equiv (E_t^n, \vec{p}_t^n)$ at the moment of the collision was derived from the measured spectator four momentum $\mathbb{P}_{sp} \equiv (E_{sp}, \vec{p}_{sp})$ according to the following formulae: $E_t^n = m_d - E_{sp}$, and $\vec{p}_t^n = -\vec{p}_{sp}$, where m_d denotes the mass of the deuteron. The absolute momentum of the beam proton was determined based on the known beam optics and the frequency measurement of the circulating beam [25]. The outgoing proton from the $pn \rightarrow pnX$ reaction was separated from the beam in the magnetic field of the dipole and it was identified by the independent measurement of its momentum and velocity using drift chambers and scintillators. The momentum of outgoing proton was reconstructed with a precision of 6 MeV/c (standard deviation) [5] by tracing its trajectory in the magnetic field of the dipole back to the interaction point. The outgoing neutron was measured by means of the neutral particle detector, which delivered information about the position and time at which the registered neutron induced a hadronic reaction. Finally, the η meson was identified via the missing mass technique, where the four-momentum of an unobserved object produced in the quasi-free $pn \rightarrow pnX$ reaction was determined as: $\mathbb{P}_X = \mathbb{P}_t^n + \mathbb{P}_{beam} - \mathbb{P}_{proton} - \mathbb{P}_{neutron}$. The evaluation of the four-momentum vectors of the outgoing neutron and the spectator proton as well as the functioning of detectors used for their registration will be described more detailed in the following sections. Whereas for the detailed description of other detectors used in this experiment the reader is referred to the previous publications of the COSY-11 group [26].

2.1 Neutron detector

The neutral particle detector is positioned at a distance of 7.36 m from the interaction region. It consists of 24 modules, each built out of 11 plastic scintillator plates interlayed by 11 plates of lead each with dimensions of $270 \times 90 \times 4$ mm³ [31,33]. Each detection unit is read out on its upper and lower edge by photomultipliers. The modules are arranged into five layers as it is schematically shown in Fig. 1. In front of the first layer, in order to permit a separation between charged and neutral particles, an additional scintillator counter (often referred to as a veto detector) built out of four overlapping modules with dimensions of $400 \times 200 \times 4$ mm³ has been positioned [34]. The determination of the four momentum of the neutron is based on the time of flight between the interaction point and the hit position in the neutral particle detector [31,33,34]. The time of the reaction is deduced from the measurements of the proton velocity, its trajectory and the time when it crossed the S1 counter. The obtained distribution of the time of flight is

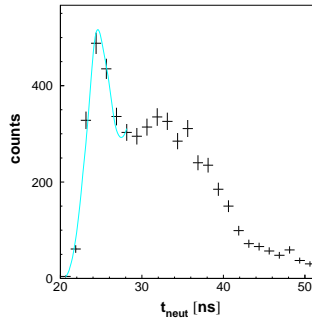


Fig. 2. Distribution of the time-of-flight measured between the target and the neutral particle detector.

presented in Fig. 2. A clear peak around 24.5 ns is associated to the γ quanta originating from decays of e.g. π^0 mesons which are produced copiously in the proton-deuteron reactions. For the $pn \rightarrow pn\eta$ reaction, at a beam momentum of $p_{beam} = 2.075$ GeV/c, the time of flight expected for neutrons is larger than 32 ns. The identification of neutron allowed to determine its energy and momentum vector based on the time-of-flight and the hit position, the latter was defined as the center of that module whose signal was produced as a first one.

2.2 Spectator detector

For the determination of the kinetic energy and scattering angle of the spectator protons a dedicated silicon detector system has been used [35]. It consists of four double-layered modules each with a thickness of $300 \mu\text{m}$. The front layer (the one closer to the beam) contains 18 silicon strips each with an active area of $20 \times 5 \text{ mm}^2$, while the back layer contains 6 silicon strips with active area of $20 \times 18 \text{ mm}^2$. A schematic view of the spectator detector arrangement is presented in Fig. 1. The modules are positioned at a distance of about 5 cm from the interaction region and their active area covers about 22% of the full solid angle. The arrangement was a compromise between the maximum coverage of the solid angle, angular resolution and the technical needs for the installation [23,31]. The detector has been used previously for experiments at the CELSIUS storage ring by the PROMICE/WASA collaboration [35]. Figure 3 presents observed spectra of the energy losses deposited in the front layer of the silicon detector (dE axis) versus the energy deposition in the back layer (E axis) for two pairs (out of 72 pairs) positioned at different distances from the interaction region. Both distributions show clear bands from the low energy protons. Differences in shapes of the proton bands in the left and right panel of Fig. 3 are due to the fact that the effective thickness of the silicon pads as seen by the particles outgoing from the interaction region varies as a function of the particle's emission angle. These variations allowed to check the position

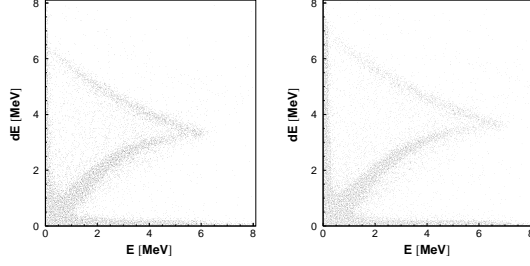


Fig. 3. dE–E plot for events registered in the spectator silicon detector for two pairs placed under different angles with respect to the interaction region. Signals from deuterons are not observed since deuterons cannot be emitted towards the detector (upwards to the proton beam) due to the kinematics.

and orientation of the spectator detector relative to the interaction region. For this aim we have compared the experimental dE–E distributions to the spectra simulated for different positions of the specator detector. By examining the χ^2 distribution we have determined the arrangement of modules with an accuracy of ± 1 mm, consistent with the nominal values based on the geometrical design of the setup. The accuracy of ± 1 mm is fully sufficient in view of the size of the stream of the deuteron target with a diameter of 9 mm [27].

2.3 Determination of the excess energy and the production yields

A spectrum of the momenta of particles identified as spectator protons, as measured in this experiment, is shown in the left panel of Fig. 4. In addition to the data points, this figure shows a superimposed histogram depicting expectations derived assuming that the momentum distribution of nucleons inside the deuteron is given by the Paris nucleon-nucleon potential [36]. A good agreement between the experimental and simulated spectra raised the confidence to the method used. In the experiment we were able to register the spectator protons with momenta ranging from 50 MeV/c to circa 115 MeV/c. The energy losses for protons with momenta lower than 50 MeV/c are not separable from the noise range and the spectators with momenta higher than 115 MeV were not taken into account since in the analysis we used the back layer of the spectator detector as a veto for the reduction of signals from charged pions. The noise cut has been performed for each silicon pad separately, analysing the spectra of energy loss triggered by a pulser with a frequency of 1 Hz used concurrently with other experimental triggers.

The measurement of the spectator momentum and as a consequence the determination of the total energy for the quasi-free proton-neutron collisions allowed to establish the excess energy Q with respect to the $pn \rightarrow pn\eta$ process for each event. The determined experimental distribution is shown in the right panel of Fig. 4. Its shape results from i) the genuine excitation function for

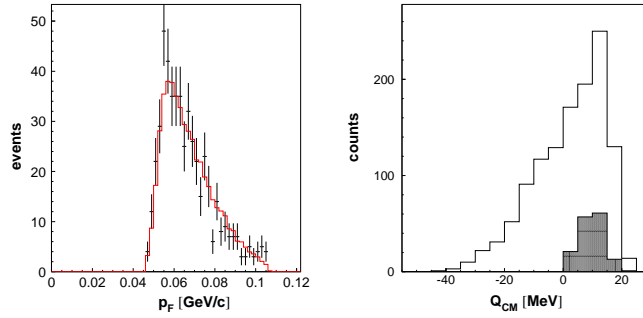


Fig. 4. (left) Points with error bars denote experimental distribution of the momentum of the spectator protons. Full line represents the Monte-Carlo spectrum of the spectator momentum resulting from the Fermi momentum distribution [36] of nucleons inside the deuteron convoluted with the acceptance and efficiency of the COSY-11 detector setup. (right) Experimental distribution of the excess energy Q with respect to the $pn\eta$ system determined for the $pn \rightarrow pnX$ reaction (solid line) and for the $pn \rightarrow pn\eta$ events (shaded histogram).

the η meson and the multi-meson production in the proton-neutron collision, ii) from the Fermi momentum distributions of the nucleons in the deuteron target, and iii) from the acceptance and efficiency of the COSY-11 apparatus.

For negative excess energies Q the η meson cannot be created and hence all events for $Q < 0$ originate from the quasi-free pions production. For positive Q additionally to the production of pions also the $pn \rightarrow pn\eta$ reaction can occur. This, however cannot be identified on the event by event basis since the COSY-11 detector system does not allow for the efficient registration of the decay products of the produced mesons. Therefore, in order to disentangle between pions and the η meson production we have grouped the collected data according to the excess energy and for each sample the number of $pn \rightarrow pn\eta$ reaction was extracted based on the missing mass distribution. Optimizing the statistics and resolution, the range of excess energy above the η meson production threshold has been divided into intervals of $\Delta Q = 5$ MeV width. The width of the bin corresponds to the accuracy (FWHM) of the determination of the excess energy which was estimated based on Monte-Carlo simulations taking into account the size of the target, the spread of the beam momentum as well as the horizontal ($\sigma(x) \approx 2$ mm) and vertical ($\sigma(y) \approx 4$ mm) beam size [37]. As a result for the $pn \rightarrow pn\eta$ reaction near the threshold we derived a standard deviation for the excess energy of $\sigma(Q) = 2.2$ MeV which is to be compared with 1.8 MeV obtained at similar conditions at the PROMICE/WASA setup [35].

For $Q > 0$ missing mass spectra have been established for each interval of ΔQ separately. Next, a corresponding background distribution has been constructed from all events with $Q < 0$ MeV, following the procedure described in details in a dedicated article [38].

Subsequently, to each distribution for $Q > 0$ the corresponding background spectrum has been normalized for mass values less than $0.25 \text{ GeV}/c^2$. In this missing mass region events correspond to a single pion production for which a production cross section stays nearly constant when the excess energy changes by a few tens of MeV since with respect to the single pion the energy is high above the threshold. In order to gain more confidence to the procedure we have also performed an alternative normalisation, requiring that after the background subtraction the ratio of the integral of missing mass experimental spectrum between 0.3 and $0.5 \text{ MeV}/c^2$ to the integral between $0.5 \text{ MeV}/c^2$ and the kinematical limit is the same as the corresponding ratio of integrals obtained from Monte-Carlo simulations. Both normalisation methods resulted in a statistically consistent result. As an example, the left panel of Fig. 5

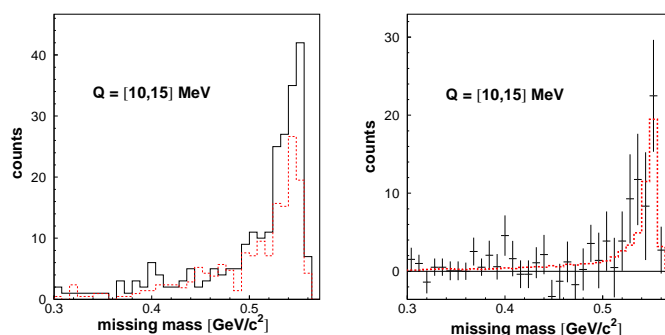


Fig. 5. (left) The solid line denotes the missing mass distribution of the $pn \rightarrow pnX$ reaction determined for the excess energy range from 10 to 15 MeV, and the dashed line shows the background distribution constructed from events with $Q < 0$ according to the method described in reference [38]. (right) Missing mass distribution of the $pn \rightarrow pn\eta$ reaction determined by subtraction of histograms from the left panel. Vertical bars indicate statistical errors only. Superimposed dashed line denotes result of simulations normalized to the data in amplitude.

shows the experimental missing mass spectra for signal (solid line) and background (dashed line) corresponding to the excess energy interval between 10 and 15 MeV. The resulting background subtracted distribution for the quasi-free $pn \rightarrow pn\eta$ reaction is presented in the right panel of Fig. 5. The number of $pn \rightarrow pn\eta$ events has been extracted from this spectrum by fitting to it the simulated distribution with the amplitude as the only free parameter. The simulation was based on the GEANT-3 code [39] containing the exact geometry of the COSY-11 detector system as well as the precise map of the magnetic field of the dipole magnet. Also the momentum and spatial beam spreads, multiple scattering of particles, and other known physical and instrumental effects have been taken into account [7,26,37]. The calculations take into account also the proton-neutron final state interaction [31] which changes the acceptance by 5%. Finally, in order to obtain the missing mass spectrum (dashed line in Fig. 5 (right)) a simulated detector response was analyzed in the same way as the experimental data.

2.4 Luminosity

The reference reaction used for the purpose of calculating the luminosity was the quasi-free elastic scattering of protons. The measurement was based on the registration of the momentum vector of the forward scattered proton and the direction of motion of the recoil proton. The recoil protons were registered in the scintillator counter S4 and the granulated silicon detector Si_{mon} , while the forward scattered protons were registered by the stack of drift chambers D1 and D2, and the scintillator array S1 (see Fig. 1). For triggering the coincidence between signals from S1 and S4 scintillators was required. Events corresponding to the elastically scattered protons have been identified on the basis of the distributions of the transversal versus the parallel momentum components of the forward scattered proton, on which a signal from the $pp \rightarrow pp$ reaction appears as a clear enhancement of the density of events around the expected kinematical ellipse [37,40]. In order to determine the integrated luminosity, numbers of elastically scattered protons registered in modules of the S1 detector were compared to the inner products of the differential cross sections and the probability density of the distribution of the Fermi momentum computed for the solid angles covered by the relevant S1 detection units. For more detailed description the interested reader is referred to the dedicated article [40]. The values of integrated luminosity determined in four independent detection modules of the S1 detector are statistically consistent with the average amounting to: $L = (208 \pm 3) \cdot \text{nb}^{-1}$, where the quoted error stands for the statistical uncertainty only.

3 Results

Total cross sections determined for the quasi-free $pn \rightarrow pn\eta$ reaction are given in Table 1 and are presented in the left panel of Fig. 6. Vertical error bars Table 1

Total cross sections for the $pn \rightarrow pn\eta$ reaction as a function of the excess energy. Given are the statistical and systematic uncertainties, respectively. The energy intervals correspond to the binning applied.

Q [MeV]	σ [μb]
(0,5]	$1.06 \pm 0.42 \pm 0.21$
(5,10]	$3.81 \pm 0.74 \pm 0.76$
(10,15]	$10.4 \pm 2.6 \pm 2.1$
(15,20]	upper limit of 13.7 at 90% CL

shown in Fig. 6 denote the statistical uncertainty only, while the horizontal

bars represent the size of the excess energy bins for which the total cross section values were extracted. In addition the total systematical uncertainty was estimated to be about 20%. It originates from ten independent contributions which were added in quadrature, and which were estimated by varying (in the analysis of the data and simulations of the acceptances) the values of parameters used for the description of the experiment. The studies revealed that: i) changing the global time offset of the neutron detector, within one standard deviation of its statistical uncertainty, results in a change of the cross sections by $\pm 5\%$, ii) the variation of the cut on the noises in the spectator detector within the limits of energy resolution resulted in an error of $\pm 7\%$, iii) changing the position of the spectator within the range of expected uncertainty (± 1 mm) resulted in an error of $\pm 15\%$, iv) varying in simulations the beam momentum resolution arbitrarily by ± 1 MeV/c around its nominal value of 3.5 MeV/c resulted in changes of cross sections values by $\pm 3\%$, v) the changes in simulations of the time resolution of the neutron detector (0.4 ns) by ± 0.2 ns gave $\pm 5\%$ error in the cross section. Additionally we have also taken into account an uncertainty due to the method used for the background subtraction amounting to 3% [38], and systematic errors of the luminosity determination discussed and estimated in details in reference [40], where it was established that the significant contributions originate from the method of the background subtraction (3%), and from the overall normalisation error of the reference data (4%) [41]. We took also into account uncertainty of $\pm 2\%$ [31] connected to the calculations of the Fermi momentum distribution. This uncertainty was established as the difference between results determined using the Paris [36] and the CDBONN [42] potentials. The other important effect considered is the reabsorption of the produced meson by the spectator proton which is proportional to the average of the inverse square of the distance between two nucleons in the deuteron and which reduces the cross section by a factor of about 3% [43]. Therefore we increased the determined cross sections by a factor of 1.03 assuming conservatively the uncertainty of this correction to be not larger than $\pm 1\%$ of the cross section. Another nuclear effect decreasing the total cross section by about 4.5% [2], referred to as the “shadow effect”, was not taken into account because the reduction of the beam flux seen by the neutron, due to the shielding by a spectator proton, is expected to be the same for the quasi-elastic scattering which was used for the determination of the luminosity.

Finally the uncertainty of the detection efficiency, predominantly due to the uncertainty in the efficiency of the neutron registration, is estimated to be not larger than $\pm 5\%$. The computation of the efficiency and acceptance of the COSY-11 detection system is based on the GEANT-3 [39] simulation packages which uses the GEANT-FLUKA subroutines for the calculations of the hadronic interactions. For the beam momentum of 2.075 GeV/c and the conditions of the detection with the COSY-11 setup the kinetic energy of neutrons from the $pd \rightarrow p_{sp}pn\eta$ reaction ranges from 200 to 430 MeV. The resulting

efficiency of the 44 cm thick COSY-11 neutral particle detector varies in this neutron energy range from 51% to 56% [34]. This is in a very good agreement with expectations based on the efficiencies determined for LAND [44] and other calorimeters [34,45].

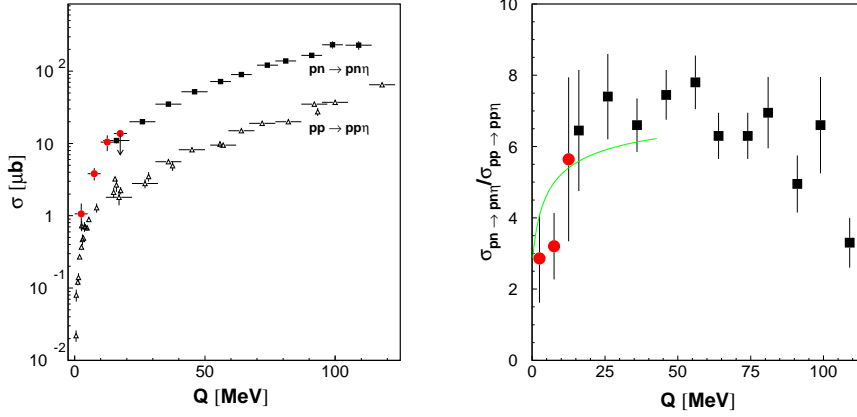


Fig. 6. (Left) Excitation functions for the near threshold η meson production via reactions $pn \rightarrow pn\eta$ (filled symbols) and $pp \rightarrow pp\eta$ (open symbols) [1,2,3,4,5,6]. Results of this article, presented as full circles, are consistent with values of cross sections determined by the CELSIUS/WASA group (filled squares) [15]. (Right) Ratio of the total cross sections for the $pn \rightarrow pn\eta$ and $pp \rightarrow pp\eta$ reactions. A superimposed line indicates a result of the fit taking into account the final state interaction of nucleons.

The right panel in Fig. 6 shows the ratio of the total cross sections for the $pn \rightarrow pn\eta$ and $pp \rightarrow pp\eta$ reactions plotted as a function of the excess energy. It can be seen that this ratio falls down at lower values of Q . To large extent, this behavior may plausibly be explained by the difference in strength of the proton-proton and proton-neutron FSI [46]. An influence of the nucleon-nucleon interaction on the shape of the excitation function for the $pn \rightarrow pn\eta$ and $pp \rightarrow pp\eta$ reactions may be well described by the closed analytical formula derived by Fäldt and Wilkin [47,48] which implies that:

$$\frac{\sigma(pn \rightarrow pn\eta)}{\sigma(pp \rightarrow pp\eta)} = 0.5 + C \left(\frac{\sqrt{\epsilon_{pp}} + \sqrt{\epsilon_{pp} + Q}}{\sqrt{\epsilon_{pn}} + \sqrt{\epsilon_{pn} + Q}} \right)^2, \quad (1)$$

where $\epsilon_{pn} = 2.2$ MeV and $\epsilon_{pp} = 0.68$ MeV [49] are the corresponding “binding” energies of the pn bound and pp virtual states, respectively [47]. We have fitted the function given by equation 1 (with C as the only free parameter) to the data in the excess energy range from 0 to 40 MeV where the higher partial waves of the proton-proton system are suppressed [7]. The result is presented in Fig. 6 as the solid line and explained to some extent the observed decrease of the ratio at threshold.

4 Summary

Using the COSY-11 detector setup we have conducted measurements of the total cross sections for the quasi-free $pn \rightarrow pn\eta$ reaction in the very close-to-threshold region. The experiment has been performed investigating the η meson production on a neutron bound in a deuteron target. The quasi-free proton-neutron reactions were tagged by the registration of the spectator proton. The Fermi momentum distribution of the nucleons inside the deuteron has been accounted for in the calculations of the integrated luminosity as well as in the determination of the total cross section. The derived total cross sections are consistent in the overlapping excess energy range with the previous measurement performed by the CELSIUS/WASA group. At the threshold the determined total cross section for the $pn \rightarrow pn\eta$ process exceeds the total cross section for the $pp \rightarrow pp\eta$ reaction by a factor of three in contrast to the factor of six observed for higher excess energies. The observed decrease may be assigned to some extent to the different energy dependence of the proton-proton and proton-neutron final state interactions [46]. A slight bump-like structure in the ratio of the $pn \rightarrow pn\eta$ to $pp \rightarrow pp\eta$ cross sections with a flat maximum at an excess energy of about 50 MeV could be due to the resonance $N^*(1535)$ ($m(N^*) - m_\eta - m_{nucleon} \approx 49$ MeV) indicating that coupling of this resonance to the neutron- η can be stronger than to the proton- η channel.

5 Acknowledgements

We are grateful to Colin Wilkin for many useful discussions and for the interpretation of the decrease of the cross sections ratio. We acknowledge the great help when installing the neutron and spectator detectors received from E. Białkowski, O. Felden, G. Friori, W. Migdał, and D. Protić. The work was partially supported by the European Community-Research Infrastructure Activity under the FP6 programme (Hadron Physics, RII3-CT-2004-506078), by the Polish Ministry of Science and Higher Education under grants No. 3240/H03/2006/31 and 1202/DFG/2007/03, and by the German Research Foundation (DFG).

References

- [1] J. Smyski et al., Phys. Lett. B **474** (2000) 182; A. M. Bergdolt et al., Phys. Rev. D **48** (1993) 2969.
- [2] E. Chiavassa et al., Phys. Lett. B **322** (1994) 270.

- [3] H. Calén et al., Phys. Lett. B **366** (1996) 39.
- [4] H. Calén et al., Phys. Rev. Lett. **79** (1997) 2642.
- [5] P. Moskal et al., Phys. Rev. C **69** (2004) 025203.
- [6] F. Hibou et al., Phys. Lett. B **438** (1998) 41.
- [7] P. Moskal, arXiv: hep-ph/0408162.
- [8] A. Khoukaz et al., Eur. Phys. J. A **20** (2004) 345; P. Moskal et al., Phys. Lett. B **474** (2000) 416; F. Balestra et al., Phys. Lett. B **491** (2000) 29; P. Moskal et al., Phys. Rev. Lett. **80** (1998) 3202.
- [9] M. Abdel-Bary et al., Eur. Phys. J. A **16** (2003) 127.
- [10] A. Moalem et al., Nucl. Phys. A **600** (1996) 445; V. Bernard et al., Eur. Phys. J. A **4** (1999) 259.
- [11] G. Fäldt and C. Wilkin, Phys. Scripta **64** (2001) 427.
- [12] K. Nakayama et al., Phys. Rev. C **65** (2002) 045210; K. Nakayama et al., arXiv:0803.3169 [hep-ph].
- [13] S. D. Bass, Phys. Lett. B **463** (1999) 286; S. D. Bass, arXiv:hep-ph/0006348.
- [14] S. D. Bass, Phys. Scripta **T 99** (2001) 96.
- [15] H. Calén et al., Phys. Rev. C **58** (1998) 2667.
- [16] R. Czyżykiewicz et al., Phys. Rev. Lett. **98** (2007) 122003.
- [17] R. Shyam, Phys. Rev. C **75** (2007) 055201.
- [18] J-J Xie et al., arXiv:0802.2802 [nucl-th].
- [19] K. Maltman and N. Isgur, Phys. Rev. D **29** (1984) 952.
- [20] M. Abdel-Bary et al., Eur. Phys. J. A **29** (2006) 353.
- [21] M. Abdel-Bary et al., Eur. Phys. J. A **36** (2008) 7.
- [22] Y. Maeda et al., Phys. Rev. Lett. **97** (2006) 142301; S. Barsov et al., Eur. Phys. J. A **21** (2004) 521; I. Lehmann et al., Nucl. Instr. & Meth. A **530** (2004) 275; H. H. Adam et al., e-Print Archive: nucl-ex/0411038; J. Zlomanczuk et al., Phys. Rev. C **69** (2004) 014003.
- [23] P. Moskal, e-Print Archive: nucl-ex/0110001.
- [24] I. Jaegle et al., e-Print: arXiv:0804.4841.
- [25] D. Prasuhn et al., Nucl. Instr. & Meth. A **441** (2000) 167.
- [26] S. Brauksiepe et al., Nucl. Instr. and Meth. A **376** (1996) 397; P. Klaja et al., AIP Conf. Proc. **796** (2005) 160; J. Smyrski et al., Nucl. Instr. and Meth. A **541** (2005) 574.

- [27] H. Dombrowski et al., Nucl. Instr. & Meth. **A 386** (1997) 228.
- [28] M. Garçon and J. W. Van Orden, Adv. Nucl. Phys. **26** (2001) 293.
- [29] L. P. Kaptari, B. Kampfer, S.S. Semikh, J. Phys. **G 30** (2004) 1115.
- [30] F. Duncan et al., Phys. Rev. Lett. **80** (1998) 4390.
- [31] R. Czyżykiewicz, Diploma Thesis, Jagellonian University, **Jül-4017** (2002).
- [32] P. Moskal, M. Wolke, A. Khoukaz, W. Oelert, Prog. Part. Nucl. Phys. **49** (2002) 1.
- [33] J. Przerwa, e-Print Archive: hep-ex/0408016; J. Przerwa et al., AIP Conf. Proc. **950** (2007) 112.
- [34] T. Rożek, Ph. D. Dissertation, University of Silesia, **Jül-4184** (2005).
- [35] R. Bilger et al., Nucl. Instr. & Meth. **A 457** (2001) 64.
- [36] M. Lacombe et al., Phys. Lett. **B 101** (1981) 139.
- [37] P. Moskal et al., Nucl. Instr. & Meth. **A 466** (2001) 448.
- [38] P. Moskal et al., J. Phys. **G 32** (2006) 629.
- [39] CERN Program Libraries Long Writeups W5013 (1994).
- [40] P. Moskal, R. Czyżykiewicz, AIP Conf. Proc. **950** (2007) 118.
- [41] D. Albers et al., Phys. Rev. Lett. **78** (1997) 1652.
- [42] R. Machleidt et al., Phys. Rev. **C 63** (2001) 024001.
- [43] E. Chiavassa et al., Phys. Lett. **B 337** (1994) 192.
- [44] T. Blaich et al., Nucl. Instr. & Meth. **A 314** (1992) 136.
- [45] E. Amarian, Nucl. Instr. & Meth. **A 460** (2001) 239; P. A. Berardo et al., Phys. Rev. **D 6** (1972) 756; A. S. L. Parsons et al., Nucl. Instr. & Meth. **79** (1970) 43.
- [46] C. Wilkin, private communication (2008).
- [47] G. Fäldt and C. Wilkin, Phys. Lett. **B 382** (1996) 209.
- [48] G. Fäldt and C. Wilkin, Phys. Rev. **C 56** (1997) 2067.
- [49] P. Moskal et al., Int. J. Mod. Phys. **A 22** (2007) 305.